Science Advances
AAAS

Supplementary Materials for

Klp2-mediated Rsp1-Mto1 colocalization inhibits microtubule-dependent microtubule assembly in fission yeast

Lingyun Nie *et al.*

Corresponding author: Chuanhai Fu, chuanhai@ustc.edu.cn; Shengnan Zheng, zhengsn@mail.ustc.edu.cn; Kai Jiang, jiangkai@whu.edu.cn

Sci. Adv. **11**, eadq0670 (2025)
DOI: 10.1126/sciadv.adq0670

This PDF file includes:

Supplementary methods

Co-expression of γ-TuSC and Mzt1-His in insect cells

Bacmid preparation

Bacmids were generated by transforming DH10Bac competent cells with the plasmids pCF.4546 (Mzt1-His), pCF.4550 (Alp4 and Gtb1) and pCF.4551 (Alp6-TEV-MBP-His and Gtb1). The cells were plated on LB agar containing 0.4 mM IPTG, 100 μg/ml 5-bromo-3-indolyl-beta-galactoside (Bluo-Gal), 50 μg/ml kanamycin, 7 μg/ml gentamycin and 10 μg/ml tetracycline, and incubated at 37°C in the dark for 48~72 hours until blue/white colonies appeared. White colonies were picked and verified by polymerase chain reaction (PCR), and correct colonies were inoculated into 6 ml LB liquid containing 50 μg/ml kanamycin, 7 μg/ml gentamycin and 10 μg/ml tetracycline and cultured at 37°C overnight. Bacmids were isolated the next day with StarPrep Fast Plasmid Mini Kit (D201-04, GenStar).

Baculovirus production and co-expression of γ-TuSC and Mzt1-His

Sf9 insect cells were used to produce baculovirus, and High Five insect cells were used to co-express γ-TuSC and Mzt1-His. Insect cells were cultured in SIM SF Serum-Free Medium (MSF1, Sino Biological) with 1% Penicillin-Streptomycin (PS) at 27°C. The bacmids, described above, were used to produce baculovirus, which was amplified to obtain P1, P2, and P3 batches. To co-express γ-TuSC and Mzt1-His, we co-infect High Five insect cells at the log phase (1.5-2.5 × 10^6 cells/ml) with equal volumes of corresponding P3 baculoviruses. After ~72 hours of infection, the infected cells were collected by centrifugation at 700 *g* for 5 minutes.

Expression of GFP-Klp2, MCP-mCherry and MCP-GFP in HEK293T cells

Plasmids for protein expression in HEK293T cells were isolated by using QIAGEN Plasmid Plus Midi kit (12943, QIAGEN). HEK293T cells were cultured in DMEM/F12 medium (G4610, Servicebio) with 10% FBS and 1% Penicillin-Streptomycin (PS) at 37°C. Polyethylenimine (PEI) (24765, Polysciences) was used to transfect HEK293T cells, following a previous protocol (*33*). Briefly, we mixed 30 μg plasmids and 60 μl PEI (1 mg/ml) in serum-free medium and transfected cells in a 15-cm dish. After 12-24 hours, DMEM/F12 with 10% FBS and 1% Penicillin-Streptomycin were added to replace the transfection medium. We then harvested cells after 36 hours of the medium replacement.

Protein purification

Purification of γ-TuSC and Mzt1-His from insect cells

γ-TuSC, with Alp6 tagged with TEV-MBP-His, and Mzt1-His co-expressed in insect cells were purified with Amylose resins (E8021, NEB). High Five insect cells from 200 ml culture were resuspended in 30 ml pre-cooled HB100 buffer (40 mM K-HEPES, 100 mM KCl, 1 mM EGTA, 1 mM $MgCl_2$, 0.1 mM GTP, 1 mM DTT, pH 7.5) supplemented with 1 mM PMSF (Sangon), pepstatin (Sangon), and EDTA-free protease inhibitors (Roche). The resuspended cells were crushed with a high-pressure

crusher (600-700 MPa) for 5 minutes, and cell lysates were centrifuged for 45 minutes at 13,800 *g* at 4℃. The supernatant was filtered through a 0.45 μm filter and then a 0.22 μm filter. The filtered supernatant was incubated with 2 ml Amylose resins (E8021, NEB) for 4 hours at 4℃, and the Amylose resins were washed with 30-40 column volumes of HB100 buffer and eluted with HB100 buffer containing 50 mM maltose. For Amylose pull-down assays, the resins bound with γ-TuSC and Mzt1-His were kept in HB100 buffer containing 0.1% Triton X-100 and 20% glycerol and stored at -20℃.

Purification of GFP-Klp2, MCP-mCherry and MCP-GFP from HEK293T cells

StrepII-GFP-Klp2, MS2-coat protein (MCP)-mCherry StrepII and MCP-GFP StrepII were purified with streptactin resins (SA053100, Smart-Lifesciences), following a previous protocol (*33*). Specifically, HEK293T cells were resuspended in cold PBS buffer and centrifuged for 5 minutes at 188 *g* at 4℃. The cell pellets were resuspended and lysed in lysis buffer (50 mM Na-HEPES, 150 mM NaCl, 1 mM EGTA, 1 mM $MgCl_2$, 0.5% Triton X-100, pH 7.5) supplemented with 1 mM PMSF (Sangon) and EDTA-free protease inhibitors (Roche) for 30 minutes at 4℃. The cell lysate was then centrifuged for 20 minutes at 16,200 *g* at 4℃, and the supernatant was incubated with 200 μl streptactin resins for 2 hours at 4℃. After washing eight times with 1 ml lysis buffer, the resins were washed twice with 1 ml wash buffer (50 mM Na-HEPES, 150 mM NaCl, 1 mM EGTA, 1 mM $MgCl_2$, 0.05% Triton X-100, pH 7.5). Finally, proteins were eluted with 150 μl elution buffer (50 mM Na-HEPES, 150 mM NaCl, 1 mM EGTA, 1 mM $MgCl_2$, 3.75 mM desthiobiotin, 10% glycerol, 0.05% Triton X-100, pH 7.5).

Purification of Mto1-Mto2, Rsp1 and Rsp1-Ssa1 complexes from fission yeast cells

Mto1-ymScarlet-StrepII-Mto2-13Myc, Mto1-mCherry-StrepII-Mto2-13Myc, Rsp1-mCherry-StrepII and Rsp1-eGFP-StrepII-Ssa1-HA were purified from fission yeast cells with streptactin resins (SA053100, Smart-Lifesciences). These proteins were expressed using pJK148-P*nmt1* and pJK210-P*nmt1* plasmids from the *nmt1* promoter, which can be repressed by thiamine. Yeast cells were cultured in EMM5S (thiamine-free) at 30℃ and harvested at OD_{600} ~1.0. Cell pellets were frozen in liquid nitrogen and ground in liquid nitrogen with a mortar grinder RM 200 (Retsch). After grinding, cells were dissolved in lysis buffer containing 1 mM PMSF (Sangon) and EDTA-free protease inhibitors (Roche). For Mto1-Mto2, lysis buffer (50 mM Na-HEPES, 300 mM NaCl, 1 mM EGTA, 1 mM $MgCl_2$, 0.1 mM GTP, 1% Triton X-100, pH 7.5) was used; for Rsp1 and Rsp1-Ssa1, lysis buffer (50 mM Na-HEPES,150 mM NaCl, 1 mM EGTA, 1 mM $MgCl_2$, 0.1 mM ATP, 1% Triton X-100, pH 7.0) was used. We lysed the cells for 1 hour on a tube roller at 4℃ and centrifuged the lysate twice for 20 minutes at 16,200 *g* at 4℃, and the supernatant was incubated with 200 μl streptactin resins for 2 hours at 4℃.

Before elution of Mto1-Mto2, the resins were washed four times each with 1 ml wash buffer A (50 mM Na-HEPES, 300 mM NaCl, 1 mM EGTA, 1 mM $MgCl_2$, 0.1 mM GTP, 0.5% Triton X-100, pH 7.5), four times each with 1 ml wash buffer B (50

mM Na-HEPES, 150 mM NaCl, 1 mM EGTA, 1 mM $MgCl_2$, 0.1 mM GTP, 0.5% Triton X-100, pH 7.5), four times each with 1 ml wash buffer C (50 mM Na-HEPES, 150 mM NaCl, 1 mM EGTA, 1 mM $MgCl_2$, 0.1 mM GTP, 0.05% Triton X-100, pH 7.5). Finally, we eluted Mto1-Mto2 with 150 µl elution buffer (50 mM Na-HEPES, 150 mM NaCl, 1 mM EGTA, 1 mM $MgCl_2$, 0.1 mM GTP, 3.75 mM desthiobiotin, 10% glycerol, 0.05% Triton X-100, pH 7.5). For pull-down assays, the resins bound with Mto1-ymScarlet-StrepII-Mto2-13Myc were kept in wash buffer C containing 0.1% Triton X-100 and 20% glycerol and stored at -20℃. Expression of Mto2-13Myc was checked by western blotting assays with an antibody against Myc (1:2000 dilution; 13-2500, ThermoFisher).

Before elution of Rsp1 and Rsp1-Ssa1, the resins were washed eight times each with 1 ml wash buffer D (50 mM Na-HEPES, 150 mM NaCl, 1 mM EGTA, 1 mM $MgCl_2$, 0.1 mM ATP, 0.5% Triton X-100, pH 7.0) and four times each with 1 ml wash buffer E (50 mM Na-HEPES, 150 mM NaCl, 1 mM EGTA, 1 mM $MgCl_2$, 0.1 mM ATP, 0.05% Triton X-100, pH 7.0). Finally, we eluted Rsp1 and Rsp1-Ssa1 with 150 µl elution buffer (50 mM Na-HEPES, 150 mM NaCl, 1 mM EGTA, 1 mM $MgCl_2$, 0.1 mM ATP, 3.75 mM desthiobiotin, 10% glycerol, 0.05% Triton X-100, pH 7.0). Expression of Ssa1-HA was checked by western blotting assays with an antibody against HA (1:1000 dilution; 11867423001, Roche).

Purification of proteins from E.coli cells

GST, GST-Rsp1, and His-GFP-Klp2 were expressed in *E.coli* Rosetta competent cells that were transformed with pGEX-4T2 (GST), pGEX-4T2-Rsp1 (GST-Rsp1) or pGEX-6P-1-Rsp1 (GST-Rsp1), and pET28a-GFP-Klp2 (His-GFP-Klp2) plasmids, respectively. His-MBP, and His-GFP-Mal3 were expressed in *E.coli* BL21 competent cells that were transformed with pET28a-MBP and pET28a-GFP-Mal3 plasmids, respectively. Protein expression was induced with 0.5 mM IPTG at 16℃ for 16 hours when culture OD_{600} reached ~0.8.

GST-fused proteins were purified with Glutathione Sepharose 4B resins (17527902, www.cytivalifesciences.com), and His-fused proteins were purified with Ni-NTA resins (30430, Qiagen). For GST and GST-Rsp1, cell pellets were resuspended in 30 ml pre-cooled lysis buffer (20 mM Tris, 150 mM NaCl, 10 mM $MgCl_2$, 0.1 mM ATP, pH 7.0) containing lysozyme, 1 mM PMSF (Sangon), pepstatin (Sangon), and EDTA-free protease inhibitors (Roche). For His-GFP-Klp2 and His-GFP-Mal3, cell pellets were resuspended in 30 ml pre-cooled lysis buffer (50 mM NaH_2PO_4, 300 mM NaCl, 10 mM β-mercaptoethanol, 2 mM $MgCl_2$, 0.1 mM ATP, pH 8.0) containing 20 mM imidazole, lysozyme, 1 mM PMSF (Sangon), pepstatin (Sangon), and EDTA-free protease inhibitors (Roche). For His-MBP, cell pellets were resuspended in 30 ml pre-cooled HB100 buffer (40 mM K-HEPES, 100 mM KCl, 1 mM EGTA, 1 mM $MgCl_2$, 1 mM DTT, pH 7.5) containing 30mM imidazole, lysozyme, 1 mM PMSF (Sangon), pepstatin (Sangon), and EDTA-free protease inhibitors (Roche).

E.coli cells were broken with a high-pressure crusher (700-800 MPa) for 2 minutes, and the lysates were centrifuged for 30 minutes at 13,800 *g* at 4℃. The

supernatant was incubated with 500 ul Glutathione Sepharose 4B resins (17527902, www.cytivalifesciences.com) or 2 ml Ni-NTA resins (30430, Qiagen) for 2 hours at 4℃. After incubation, the resins were washed with 30-40 column volumes of lysis buffer containing 0.05% Triton X-100. Finally, we eluted proteins with lysis buffer containing 5 mM reducing glutathione for GST-fused proteins, 200 mM imidazole for His-GFP-Klp2, or 300 mM imidazole for His-GFP-Mal3 and His-MBP.

Co-immunoprecipitation and pull-down assays

Co-immunoprecipitation

Fission yeast strains expressing GFP (ectopic expression from the *cam1* promoter) and Myc proteins (endogenous expression) were inoculated in Yeast Extract (YE) medium supplemented with adenine, leucine, uracil, histidine, and lysine (0.225 g/l each, referred to as YE5S) (Formedium). Exponentially grown cells were harvested from 1 liter culture and were ground in liquid nitrogen with the mortar grinder RM 200 (Retsch). Ground cells were dissolved in TBS buffer (Tris-buffered saline, pH 7.5) containing 0.1% Triton X-100 and supplemented with cocktail protease inhibitors and 1 mM PMSF at 4℃ for 30 minutes. Cell lysates were then centrifuged at 16,200 *g* at 4℃ for 30 minutes, and the supernatants were collected for co-immunoprecipitation. Specifically, Dynabeads Protein G beads (10004D, ThermoFisher) bound with GFP antibodies (home-made, GenScript) were added to the supernatants, and the mixture was incubated at 4℃ on a rotator for 2 hours. The Dynabeads protein G beads were then washed three times with TBS buffer containing 0.1% Triton X-100 and once with TBS buffer, followed by boiling in SDS sample buffer at 100℃ for 5 minutes. Co-precipitated proteins were analyzed by western blotting with antibodies against GFP (1:2000 dilution; 600-101-215, Rockland-inc), and Myc (1:2000 dilution; 600-401-381, Rockland-inc).

Dynabeads Protein G pull-down assays

To examine the interaction between Rsp1-Ssa1 and Mto1-Mto2, an anti-tdTomato antibody (home-made, GenScript) was bound to Dynabeads Protein G beads, and the antibody-coated beads were equilibrated in HEPES buffer (50 mM HEPES, 150 mM NaCl, 1 mM EGTA, 1 mM $MgCl_2$, 0.1 mM GTP, 0.1 mM ATP, 0.1% Triton X-100, pH 7.5). In the meantime, the following sets of proteins were mixed (total volume is 200 μl) and incubated at room temperature for 30 minutes: 1) Mto1-mCherry-StrepII-Mto2-13Myc and Rsp1-GFP-StrepII-Ssa1-HA, 2) MCP-mCherry-StrepII and Rsp1-GFP-StrepII-Ssa1-HA, 3) Mto1-mCherry-StrepII-Mto2-13Myc and MCP-GFP-StrepII, and 4) MCP-mCherry-StrepII and MCP-GFP-StrepII. The antibody-coated beads were then added to the protein mixture and incubated at 4℃ for 2 hours. The beads were washed three times with 1 ml HEPES buffer and once with 1 ml HEPES buffer without Triton X-100, followed by boiling in SDS sample buffer at 100℃ for 5 minutes. The pull-down protein samples were then analyzed by SDS-PAGE and western blotting with antibodies against tdTomato (1:1000 dilution; home-made, GenScript) and GFP (1:2000 dilution; 600-101-215, Rockland-inc).

To examine the interaction between Mto1-Mto2 and γ-TuSC-Mzt1, a similar approach as stated above was employed with the following modifications. An anti-MBP antibody was bound to Dynabeads Protein G beads. The sets of protein mixture are follows: 1) Mto1-mCherry-StrepII-Mto2-13Myc and γ-TuSC-Mzt1, 2) Mto1-mCherry-StrepII-Mto2-13Myc and His-MBP, 3) MCP-mCherry-StrepII and γ-TuSC-Mzt1, and 4) MCP-mCherry-StrepII and His-MBP. The pull-down protein samples were analyzed by SDS-PAGE and western blotting with antibodies against tdTomato (1:1000 dilution; home-made, GenScript) and MBP (1:2000 dilution; AE016, ABClonal).

To examine the interaction between Rsp1-Ssa1 and γ-TuSC-Mzt1, a simlar approach as stated above was employed with the following modifications. An anti-MBP antibody was bound to Dynabeads Protein G beads. The sets of protein mixture are follows: 1) Rsp1-GFP-StrepII-Ssa1-HA and γ-TuSC-Mzt1, 2) Rsp1-GFP-StrepII-Ssa1-HA and His-MBP, 3) MCP-GFP-StrepII and γ-TuSC-Mzt1, and 4) MCP-GFP-StrepII and His-MBP. The pull-down protein samples were analyzed by SDS-PAGE and western blotting assays with antibodies against GFP (1:2000 dilution; 600-101-215, Rockland-inc) and MBP (1:2000 dilution; AE016, ABClonal).

GST pull-down assays

Glutathione Sepharose 4B resins bound with GST-Rsp1 or GST were incubated with His-GFP-Klp2 at 4℃ for 2 hours. After incubation, the resins were washed three times with TBS buffer containing 0.1% Triton X-100 and once with TBS buffer, followed by boiling in SDS sample buffer at 100℃ for 5 minutes. The pull-down protein samples were then analyzed by SDS-PAGE and western blotting assays with antibodies against GFP (1:2000 dilution; 600-101-215, Rockland-inc) and GST (1:10000 dilution; AE006, ABClonal).

Amylose pull-down assays

To test the competitive binding of γ-TuSC-Mzt1 and Rsp1-Ssa1/MCP to Mto1-Mto2, amylose resins bound with γ-TuSC-Mzt1-His were washed once with 1 ml HB100 buffer (40 mM K-HEPES, 100 mM KCl, 1 mM EGTA, 1 mM $MgCl_2$, 0.1 mM GTP, 0.1 mM ATP, 0.5% Triton X-100, pH 7.5) and incubated with the following sets of proteins: 1) Mto1-ymScarlet-StrepII-Mto2-13Myc alone, 2) Mto1-ymScarlet-StrepII-Mto2-13Myc and Rsp1-GFP-StrepII-Ssa1-HA, or 3) Mto1-ymScarlet-StrepII-Mto2-13Myc and MCP-GFP-StrepII, in HB100 buffer at 4℃ for 1.5 hours. After incubation, the resins were washed three times with 1 ml HB100 buffer and once with 1 ml HB100 buffer without Triton X-100, followed by boiling in SDS sample buffer at 100℃ for 5 minutes. The pull-down protein samples were then analyzed by SDS-PAGE and western blotting with antibodies against tdTomato (1:1000 dilution; home-made, GenScript), Myc (1:2000 dilution; 13-2500, ThermoFisher), GFP (1:2000 dilution; 600-101-215, Rockland-inc) and γ-Tubulin (1:1000 dilution; T5326, Sigma-Aldrich).

Streptactin pull-down assays

To test the competitive binding of Klp2/Mal3 and Mto1-Mto2 to Rsp1, the streptactin resins bound with Mto1-ymScarlet-StrepII-Mto2-13Myc were washed once with 1 ml HEPES buffer (50 mM HEPES, 150 mM NaCl, 1 mM EGTA, 1 mM $MgCl_2$, 0.1 mM GTP, 0.1 mM ATP, 0.1% Triton X-100, pH 7.5) and blocked with HEPES buffer containing 0.5% non-fat milk at 4℃ for 1 hour (*34*). In the meantime, GST-Rsp1 was incubated with His-GFP-Klp2 or His-GFP-Mal3 at 25℃ for 30 minutes. The protein mixture and GST-Rsp1 alone were then added to the streptactin resins and incubated at 4℃ for 1.5 hours. After incubation, the resins were washed three times with 1 ml HEPES buffer and once with 1 ml HEPES buffer without Triton X-100, followed by boiling in SDS sample buffer at 100℃ for 5 minutes. The pull-down protein samples were then analyzed by SDS-PAGE and western blotting assays with antibodies against tdTomato (1:1000 dilution; home-made, GenScript), Myc (1:2000 dilution; 13-2500, ThermoFisher), GFP (1:2000 dilution; 600-101-215, Rockland-inc), and GST (1:2000 dilution; AE006, ABClonal).

Cold treatment experiments to depolymerize microtubule

For microtubule regrowth assay, cells were placed on ice in Eppendorf tubes for 30 minutes to depolymerize microtubules, and then shifted to a shaking water bath at 25℃ to allow microtubule polymerization (*17*). Finally, cells were rapidly fixed with 100% methanol, and then shifted to -80℃ for 15 minutes. Before imaging, the fixed cells were washed with phosphate buffered saline.

Supplementary Figures

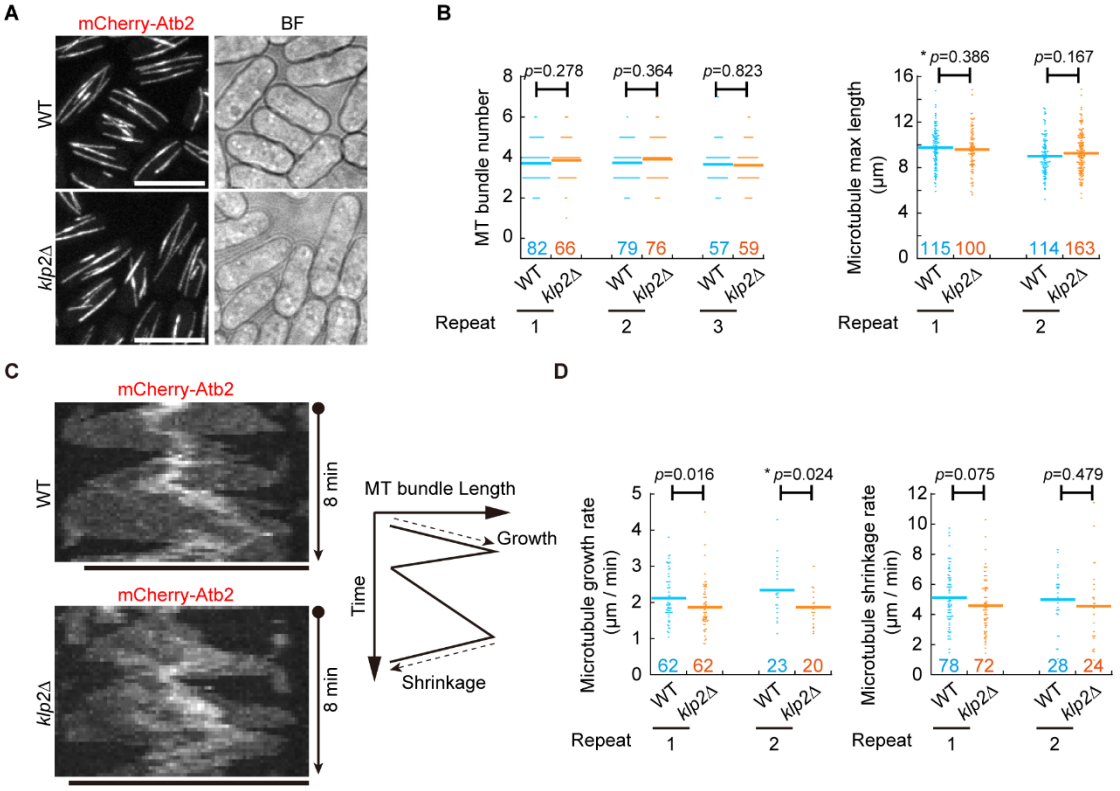

Fig. S1. The absence of Klp2 does not alter the number, maximum length, and shrinkage rate of microtubule bundles but decreases the growth rate of microtubule bundles (related to Fig. 2). (**A**) Maximum projection images of WT and *klp2*Δ cells expressing mCherry-Atb2. Scale bar, 10 μm. (**B**) Quantification of microtubule bundle number on the left and the maximum length of microtubule bundles on the right. Three or two independent experiments were performed (indicated by *repeat*), and the number of cells or microtubule bundles analyzed is indicated. The *p* values were calculated by the Wilcoxon-Mann-Whitney Rank Sum test, and the asterisk marks the *p* value calculated by Student's *t*-test. Bars represent the mean. (**C**) Kymograph graphs of mCherry-Atb2 in WT and *klp2*Δ cells. Diagrams on the right illustrates microtubule dynamics. Scale bar, 10 μm. (**D**) Quantification of the growth and shrinkage rates of microtubule bundles. Two independent experiments were performed (indicated by *repeat*). The number of growth or shrinkage events analyzed is indicated. The *p* values were calculated by the Wilcoxon-Mann-Whitney Rank Sum test, and the asterisk marks the *p* value calculated by Student's *t*-test. Bars represent the mean.

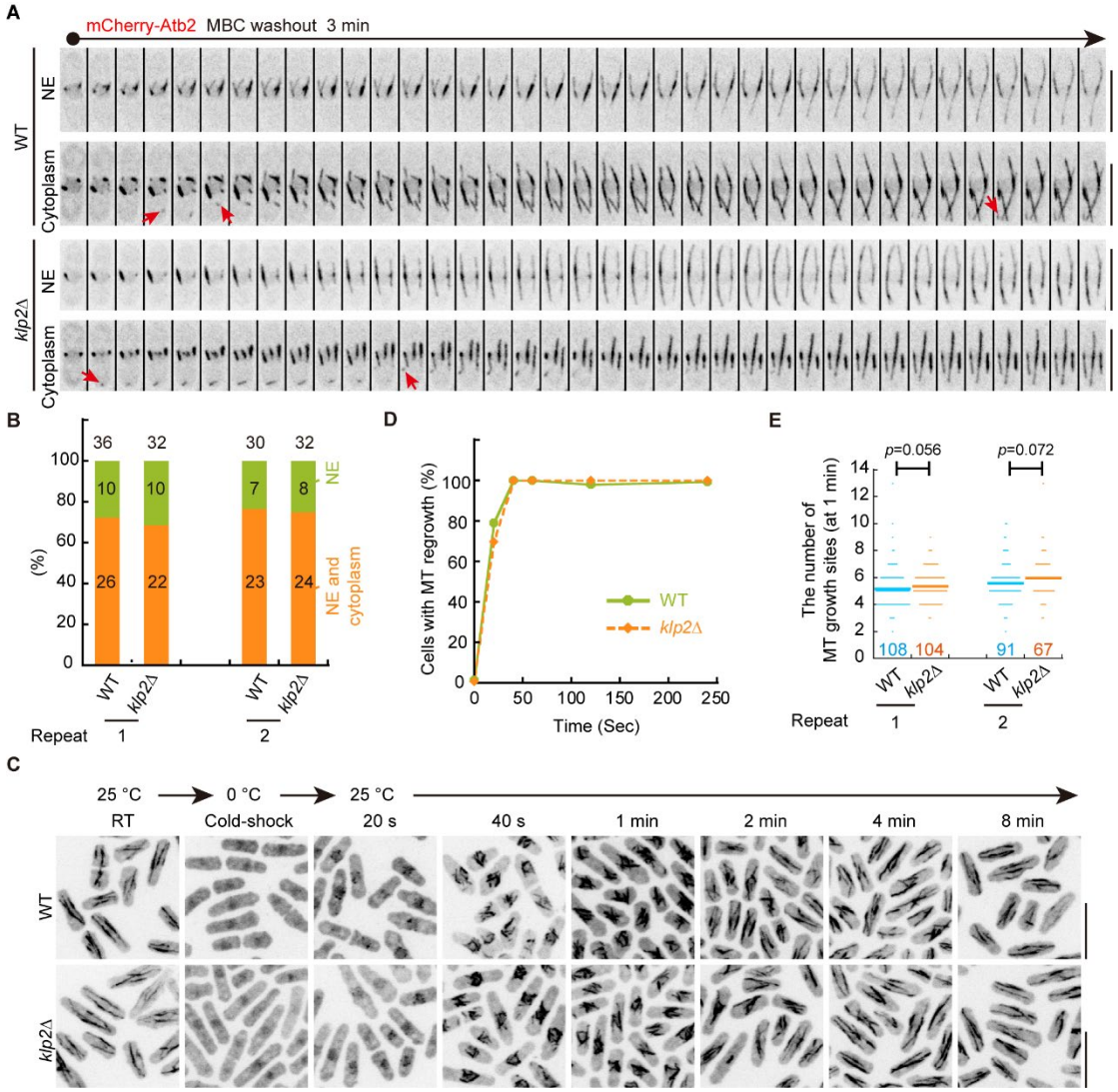

Fig. S2. The absence of Klp2 does not affect microtubule regrowth after the recovery from MBC and cold treatments (related to Fig. 4). (**A**) Time-lapse images of WT and *klp2*Δ cells expressing mCherry-Atb2. To observe microtubule regrowth in the first place, cells were treated with the microtubule-depolymerizing drug MBC and were imaged upon MBC washout. Microtubules regrew from the nuclear envelope and the cytoplasm (indicated by red arrows) in both WT and *klp2*Δ cells. Scale bar, 10 μm. (**B**) Percentage of microtubule regrowth from the nuclear envelope and/or the cytoplasm of WT and *klp2*Δ cells in (A). Two independent experiments were performed (indicated by *repeat*), and the number of cells analyzed is indicated. (**C**) Microtubule regrowth after recovery from cold treatment. WT and *klp2*Δ cells expressing mCherry-Atb2 were incubated on ice for 30 minutes to depolymerize microtubules, and were then shifted to 25°C and fixed by methanol at the indicated times. Maximum projection images are shown. Scale bar, 10 μm. (**D**) Percentage of WT and *klp2*Δ cells in (C) displaying regrowing microtubules after the release from cold treatment. A representative result from two independent experiments is shown. (**E**) Quantification of the number of sites of microtubule regrowth after 1-minute release from cold treatment for cells in (C). Two independent experiments were performed (indicated by *repeat*), and the number of cells analyzed is indicated. The *p* values were calculated by the Wilcoxon-Mann-Whitney Rank Sum test, and the bars represent the mean.

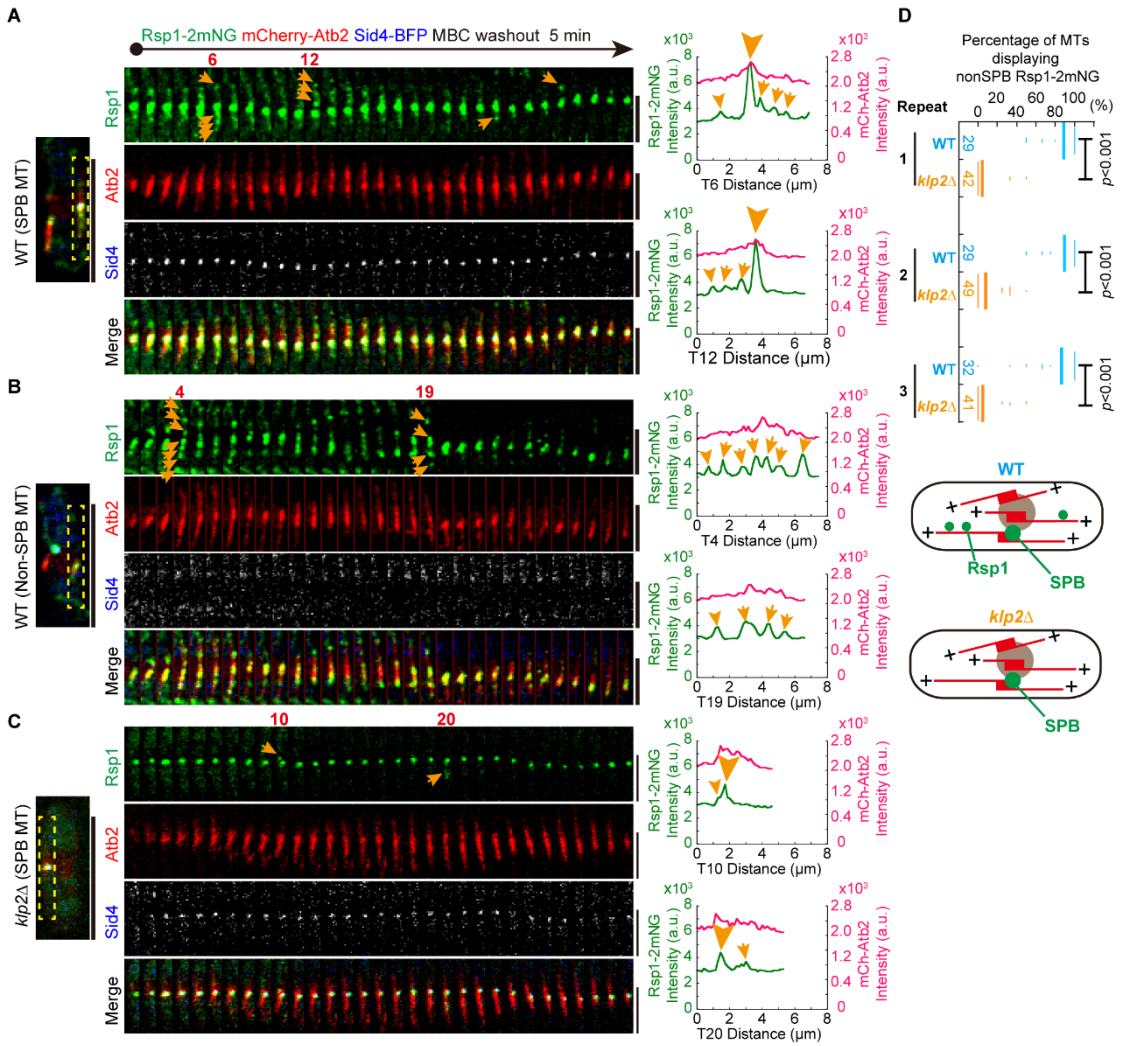

Fig. S3. Klp2 recruits Rsp1 to the microtubule lattice (related to Fig. 5). (**A**) Time-lapse images of WT cells expressing Rsp1-2mNeonGreen, mCherry-Atb2 and Sid4-mTagBFP. To observe microtubule growth in the first place, cells were treated with the microtubule-depolymerizing drug MBC and were imaged upon MBC washout. Note that on the growing microtubule carrying a SPB in the WT cell, Rsp1-2mNeonGreen (orange arrows) emerged upon microtubule growth resumed. The dashed yellow rectangle indicates the region used to create the montage images. Linescan intensity profiles of Rsp1-2mNeonGreen and mCherry-Atb2 along the indicated microtubule at the indicated timepoints are shown on the right. Orange arrows indicate non-SPB-localized Rsp1 puncta on microtubule bundles while the arrowhead indicates the SPB-localized Rsp1. Scale bars: 10 μm (whole cell image on the left), and 5 μm (montage images on the right). (**B**) Similar data as (A) are shown except that the microtubule analyzed does not carry a SPB. (**C**) Time-lapse images of *klp2*Δ cells expressing Rsp1-2mNeonGreen, mCherry-Atb2 and Sid4-mTagBFP after the release from MBC treatment. A static SPB-localized Rsp1 and few non-SPB localized Rsp1-2mNeonGreen emerged on the regrowing microtubule in *klp2*Δ cells. Scale bars: 10 μm (whole cell image on the left), and 5 μm (the montage images on the right). (**D**) Quantification of percentage of microtubules (in a cell) displaying non-SPB-localized Rsp1-2mNeonGreen, as illustrated in the diagrams below. Three independent experiments were performed (indicated by *repeat*). The number of cells analyzed is indicated. The *p* values were calculated by the Wilcoxon-Mann-Whitney Rank Sum test, and the bars represent the mean.

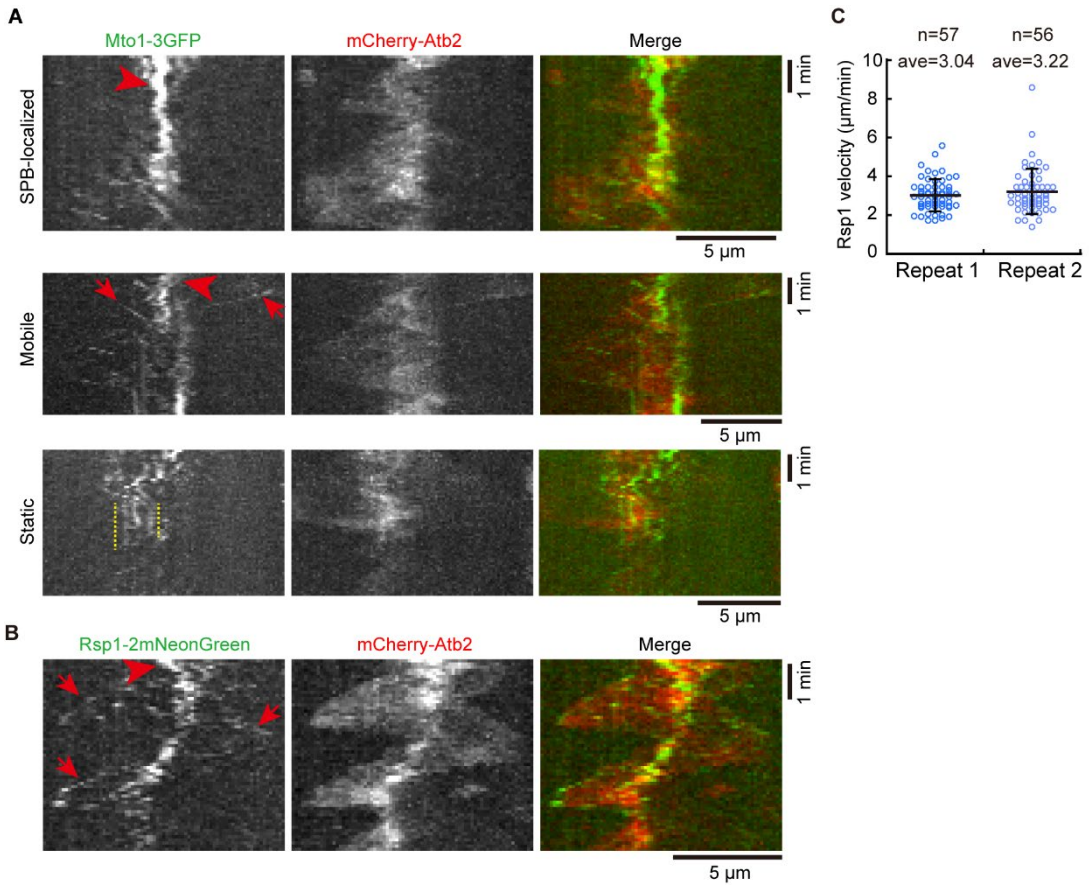

Fig. S4. The localization dynamics of Mto1 and Rsp1 (related to Fig. 5). (**A**) Kymograph graphs of Mto1-3GFP and mCherry-Atb2 in WT cells. Red arrowheads and arrows indicate SPB-localized and mobile Mto1-3GFP, respectively. Dashed yellow lines indicate static Mto1 foci localized near the microtubule minus-ends. Scale bar, 5 μm. (**B**) Kymograph graphs of Rsp1-2mNeonGreen and mCherry-Atb2 in WT cells. Red arrowhead and arrows indicate SPB-localized and mobile Rsp1-GFP, respectively. Some static Rsp1-GFP foci are detectable on the microtubule lattice. Scale bar, 5 μm. (**C**) Plot of the velocity of mobile Rsp1 in (B). Two independent experiments were performed (indicated by *repeat*). The number of Rsp1 foci analyzed is indicated, and the error bars represent S.D. The bars are the mean.

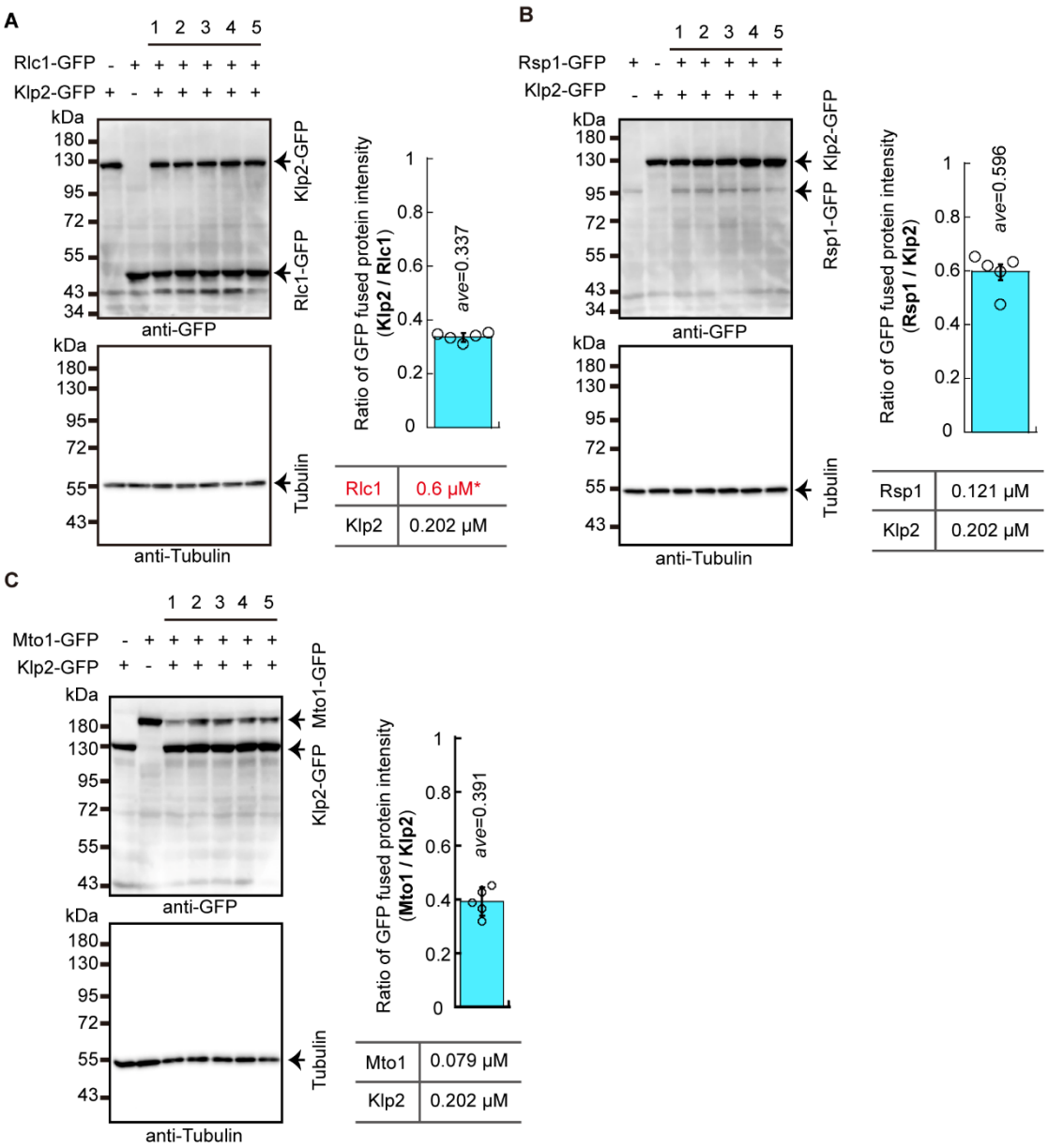

Fig. S5. The molecular stoichiometry of Klp2, Rsp1, and Mto1 (related to Fig. 6). (**A**) Expression of Klp2-GFP and Rlc1-GFP in WT cells. Antibodies against GFP and Tubulin were used for the western blotting assays. Five sets of samples were analyzed. The intensity ratio of Klp2-GFP over Rlc1-GFP was quantified on the right. The concentration of Rlc1 within a cell was determined to be 0.6 μM (*30*). Based on the molecular stoichiometry of Klp2-GFP : Rlc1-GFP (0.337 : 1) determined here, the concentration of Klp2-GFP is approximate 0.202 μM within a cell. (**B**) Expression of Klp2-GFP and Rsp1-GFP in WT cells. Antibodies against GFP and Tubulin were used for the western blotting assays. Five sets of samples were analyzed. The intensity ratio of Klp2-GFP over Rsp1-GFP was quantified on the right. Based on the molecular stoichiometry of Klp2-GFP : Rsp1-GFP (1 : 0.596) determined here, the concentration of Rsp1-GFP is approximate 0.121 μM within a cell. (**C**) Expression of Klp2-GFP and Mto1-GFP in WT cells. Antibodies against GFP and Tubulin were used for the western blotting assays. Five sets of samples were analyzed. The intensity ratio of Klp2-GFP over Mto1-GFP was quantified on the right. Based on the molecular stoichiometry of Klp2-GFP : Mto1-GFP (1 : 0.391) determined here, the concentration of Mto1-GFP is approximate 0.079 μM within a cell.

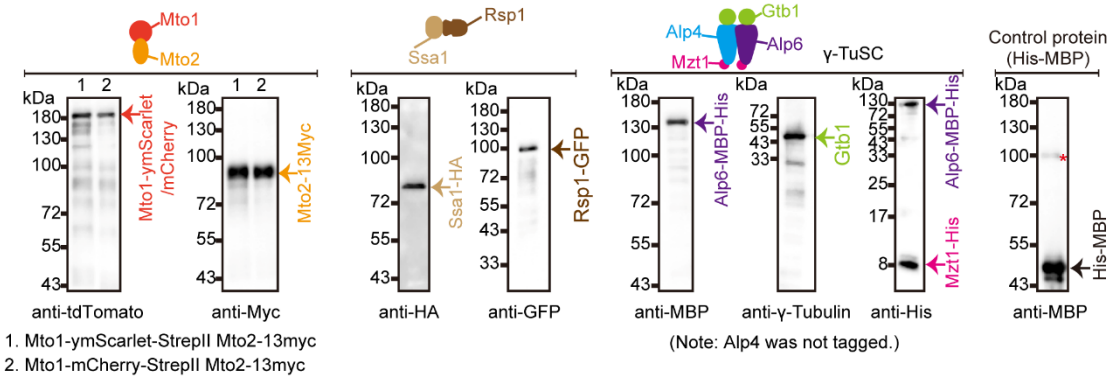

Fig. S6. Verification of purified proteins by western blotting (related to Fig. 7A). The indicated antibodies were used for the western blotting assays.

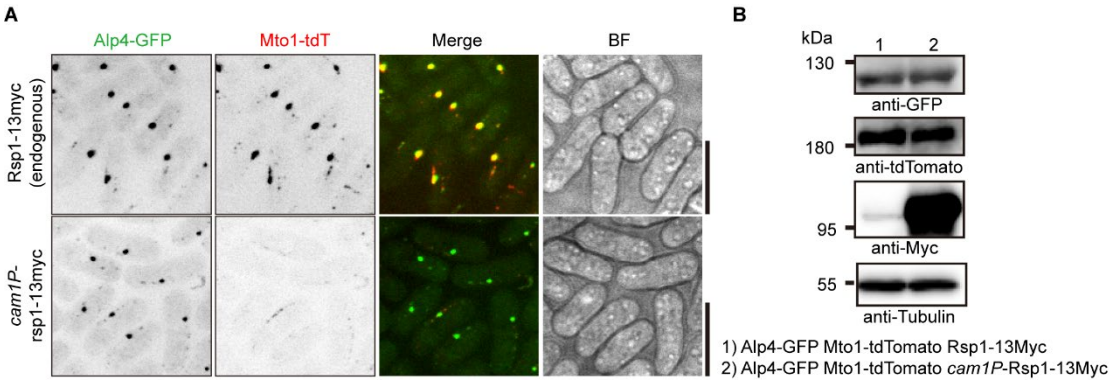

Fig. S7. Rsp1 overexpression reduces the colocalization between Mto1 and Alp4 (related to Fig. 8). (**A**) Maximum projection images of the indicated cells expressing Mto1-tdTomato and Alp4-GFP, a component of γ-TuSC. Top panel, Rsp1-13Myc was expressed from its own promoter; bottom panel, Rsp1-13Myc was expressed from the strong promoter *cam1*. Scale bar, 10 μm. (**B**) Testing the expression of Alp4-GFP, Mto1-tdTomato, and Rsp1-13Myc in the strains in (A). Antibodies against GFP, tdTomato, Myc, and Tubulin were used for the western blotting assays. The strains are shown at the bottom.

Supplementary tables

Table S1. Yeast strains

Strain	Genotype	Source
Figure 1		
CF.3948	Klp2-13myc:NatR pJK148-P*cam1*-Rsp1-GFP:*leu*+ *ade6*-M210 *ura4*-D18 h?	Lab stock
CF.10809	Klp2-13myc:NatR pJK148-P*cam1*-Rga6-GFP:*leu*+ *ade6*-M210 *ura4*-D18 h?	This study
CF.8920	Klp2-tdTomato:NatR Rsp1-2mNeongreen:HygR BFP-Atb2 *ade6*-M210 *leu1*-32 *ura4*-D18 h?	This study
CF.11487	Klp2-tdTomato:NatR Rsp1-2mNeongreen:HygR mTagBFP-Atb2:HygR *ade6*-M210? *leu1*-32 *ura4*-D18 h?	This study
Figure 2		
CF.5102	Rsp1-2mNeongreen:HygR mCherry-Atb2:HygR *ade6*-M210 *leu1*-32 *ura4*-D18 h?	Lab stock
CF.5283	*klp2*Δ:*ura*+ Rsp1-2mNeongreen:HygR mCherry-Atb2:HygR *ade6*-M210 *leu1*-32 h-	Lab stock
CF.16852	Rsp1-2mNeongreen:HygR mCherry-Atb2:HygR Sid4-mTagBFP:KanR *ade6*-M210 *leu1*-32 *ura4*-D18 h?	This study
CF.16853	*klp2*Δ:*ura*+ Rsp1-2mNeongreen:HygR mCherry-Atb2:HygR Sid4-mTagBFP:KanR *ade6*-M210 *leu1*-32 h-	This study
Figure 3		
CF.2394	Klp2-GFP:*ura*+ mCherry-Atb2:HygR *ade6*-M210? *leu1*-32 h+	Lab stock
CF.3607	*rsp1*Δ:KanR Klp2-GFP:*ura*+ mCherry-Atb2:HygR *ade6*-M210? *leu1*-32 h-	Lab stock
Figure 4		
CF.2462	Ase1-GFP:KanR mCherry-Atb2:HygR *ade6*-M210? *leu1*-32 *ura4*-D18 h+	Lab stock
CF.2431	*klp2*Δ:*ura*+ Ase1-GFP:KanR mCherry-Atb2:HygR *ade6*-M210? *leu1*-32 h+	Lab stock
Figure 5		
CF.4250	Mto1-3XGFP:KanR mCherry-Atb2:HygR *ade6*-M210? *leu1*-32 *ura4*-D18 h-	Lab stock
CF.4419	*klp2*Δ:*ura*+ Mto1-3XGFP:KanR mCherry-Atb2:HygR *ade6*-M210? *leu1*-32 h-	Lab stock
CF.5105	Rsp1-2mNeongreen:HygR Mto1-tdTomato:NatR *ade6*-M210 *leu1*-32 *ura4*-D18 h+	Lab stock
CF.8279	*klp2*Δ:*ura*+ Rsp1-2mNeongreen:HygR Mto1-tdTomato:NatR *ade6*-M210? *leu1*-32 h?	This study

Figure 6		
CF.16850	Rsp1-2mNeongreen:HygR Mto1-tdTomato:NatR mTagBFP-Atb2:HygR *ade6*-M210 *leu1*-32 *ura4*-D18 h?	This study
CF.16851	Rsp1-2mNeongreen:HygR Mto1-tdTomato:NatR Klp2-mTagBFP:KanR *ade6*-M210 *leu1*-32 *ura4*-D18 h+	This study
CF.13340	pJK148-P*nmt1*-Rsp1-mCherry StrepII:*leu*+ *ade6*-M210 *ura4*-D18 h-	This study
Figure 7		
CF.12981	pJK210-P*nmt1*-Mto1-ymScarlet StrepII:*ura*+ pJK148-P*nmt1*-Mto2-13myc:*leu*+ *ade6*-M210 h?	This study
CF.13338	pJK148-P*nmt1*-Mto1-mCherry StrepII:*leu*+ pJK210-P*nmt1*-Mto2-13myc:*ura*+ *ade6*-M210 h+	This study
CF.12986	pJK148-P*nmt1*-Rsp1-eGFP StrepII:*leu*+ pJK210-P*nmt1*-Ssa1-HA:*ura*+ *ade6*-M210 h?	This study
Figure 8		
CF.12981	pJK210-P*nmt1*-Mto1-ymScarlet StrepII:*ura*+ pJK148-P*nmt1*-Mto2-13myc:*leu*+ *ade6*-M210 h?	This study
CF.12986	pJK148-P*nmt1*-Rsp1-eGFP StrepII:*leu*+ pJK210-P*nmt1*-Ssa1-HA:*ura*+ *ade6*-M210 h?	This study
Figure S1		
CF.5433	mCherry-Atb2:HygR *ade6*-M210? *leu1*-32 *ura4*-D18 h-	Lab stock
CF.7921	*klp2*Δ:*ura*+ mCherry-Atb2:HygR *ade6*-M210? *leu1*-32 h-	Lab stock
Figure S2		
CF.5433	mCherry-Atb2:HygR *ade6*-M210? *leu1*-32 *ura4*-D18 h-	Lab stock
CF.7921	*klp2*Δ:*ura*+ mCherry-Atb2:HygR *ade6*-M210? *leu1*-32 h-	Lab stock
Figure S3		
CF.16852	Rsp1-2mNeongreen:HygR mCherry-Atb2:HygR Sid4-mTagBFP:KanR *ade6*-M210 *leu1*-32 *ura4*-D18 h?	This study
CF.16853	*klp2*Δ:*ura*+ Rsp1-2mNeongreen:HygR mCherry-Atb2:HygR Sid4-mTagBFP:KanR *ade6*-M210 *leu1*-32 h?	This study
Figure S4		
CF.4250	Mto1-3XGFP:KanR mCherry-Atb2:HygR *ade6*-M210? *leu1*-32 *ura4*-D18 h-	Lab stock
CF.16852	Rsp1-2mNeongreen:HygR mCherry-Atb2:HygR Sid4-mTagBFP:KanR *ade6*-M210 *leu1*-32 *ura4*-D18 h?	This study
Figure S5		
PT.2007	Rlc1-GFP:*ura*+ *ade6*-M210 *leu1*-32 h+	Tran Lab
CF.328	Klp2-GFP:*ura*+ *ade6*-M210 *leu1*-32 h+	Lab stock

PT.293	Rsp1-GFP:KanR *ade6*-M210 *leu1*-32 *ura4*-D18 h-	Tran Lab
PT.395	Mto1-GFP:KanR *ade6*-M210 *leu1*-32 *ura4*-D18 h+	Tran Lab
CF.16862	Klp2-GFP:*ura*+ Rlc1-GFP:*ura*+ *ade6*-M210 *leu1*-32 h?	This study
CF.16858	Klp2-GFP:*ura*+ Rsp1-GFP:KanR *ade6*-M210 *leu1*-32 h?	This study
CF.17054	Mto1-GFP:KanR Klp2-GFP:*ura*+ *ade6*-M210 *leu1*-32 h?	This study
Figure S6		
CF.12981	pJK210-P*nmt1*-Mto1-ymScarlet StrepII:*ura*+ pJK148-P*nmt1*-Mto2-13myc:*leu*+ *ade6*-M210 h?	This study
CF.13338	pJK148-P*nmt1*-Mto1-mCherry StrepII:*leu*+ pJK210-P*nmt1*-Mto2-13myc:*ura*+ *ade6*-M210 h+	This study
CF.12986	pJK148-P*nmt1*-Rsp1-eGFP StrepII:*leu*+ pJK210-P*nmt1*-Ssa1-HA:*ura*+ *ade6*-M210 h?	This study
Figure S7		
CF.17036	Alp4-GFP:KanR Mto1-tdTomato:NatR Rsp1-13myc:NatR *ade6*-M210 *leu1*-32 *ura4*-D18 h?	This study
CF.16864	Alp4-GFP:KanR Mto1-tdTomato:NatR pJK148-P*cam1*-Rsp1-13myc:*leu*+ *ade6*-M210 *ura4*-D18 h-	This study

Table S2. Plasmids

Plasmid	Genotype	Source
Figure 1		
pCF.2235	pGEX-4T2-rsp1	Lab stock
pPT.111	pGEX-4T2	Tran Lab
pTP.001	pET28a-GFP-klp2	Lab stock
pCF.2176	pJK148-P*cam1*-rsp1-GFP	Lab stock
pCF.3123	pJK148-P*cam1*-rga6-GFP	Lab stock
Figure 6		
pCF.4933	pTT5-StrepII-eGFP-klp2	This study
pCF.4611	pJK148-P*nmt1*-rsp1-mCherry-StrepII	This study
Figure 7		
pCF.4570	pJK210-P*nmt1*-mto1 (NruI site mutated)-ymScarlet StrepII	This study
pCF.4368	pJK148-P*nmt1*-mto2-13myc	This study
pCF.4602	pJK148-P*nmt1*-mto1 (NruI site mutated)-mCherry StrepII	This study
pCF.4365	pJK210-P*nmt1*-mto2 (StuI site mutated)-13myc	This study
pCF.4231	pJK148-P*nmt1*-rsp1-eGFP StrepII	This study
pCF.4565	pJK210-P*nmt1*-ssa1-HA	This study
pCF.4879	pTT5-MS2 coat protein-eGFP StrepII	This study
pCF.4880	pTT5-MS2 coat protein-mCherry StrepII	This study
pCF.4541	pFastbac Dual-Ph-BamHI-alp6 (codon optimized)-NotI	Sangon biotech (This study)

pCF.4542	pFastbac Dual-Ph-BamHI-alp4 (codon optimized)-NotI	Sangon biotech (This study)
pCF.4543	pFastbac Dual-Ph-BamHI-mzt1 (codon optimized)-NotI	Sangon biotech (This study)
pCF.4544	pFastbac Dual-P10-XhoI-gtb1 (codon optimized)-KpnI	Sangon biotech (This study)
pCF.4545	pFastbac Dual-Ph-NotI-TEV site-MBP (codon optimized)-His-PstI	Sangon biotech (This study)
pCF.4546	pFastbac1-mzt1 (codon optimized)-His	This study
pCF.4547	pFastbac Dual-Ph-alp6 (codon optimized)-TEV site-MBP (codon optimized)-His	This study
pCF.4550	pFastbac Dual-P10-gtb1 (codon optimized)-Ph-alp4 (codon optimized)	This study
pCF.4551	pFastbac Dual-P10-gtb1 (codon optimized)-Ph-alp6 (codon optimized)-TEV site-MBP (codon optimized)-His	This study
pCF.2508	pET28a-His-MBP-3C	Zang Lab
Figure 8		
pCF.4570	pJK210-P*nmt1*-mto1 (NruI site mutated)-ymScarlet StrepII	This study
pCF.4368	pJK148-P*nmt1*-mto2-13myc	This study
pCF.4231	pJK148-P*nmt1*-rsp1-eGFP StrepII	This study
pCF.4565	pJK210-P*nmt1*-ssa1-HA	This study
pCF.4879	pTT5-MS2 coat protein-eGFP StrepII	This study
pCF.4546	pFastbac1-mzt1 (codon optimized)-His	This study
pCF.4550	pFastbac Dual-P10-gtb1 (codon optimized)-Ph-alp4 (codon optimized)	This study
pCF.4551	pFastbac Dual-P10-gtb1 (codon optimized)-Ph-alp6 (codon optimized)-TEV site-MBP (codon optimized)-His	This study
pCF.4910	pGEX-6P-1-rsp1	This study
pCF.665	pET28a-his-eGFP-mal3	Lab stock
pCF.4917	pET28a-his-eGFP-klp2	This study
Figure S6		
	Same as Figure 7	
Figure S7		
pCF.4233	pJK148-P*cam1*-rsp1-13myc	This study

REFERENCES AND NOTES

1. J. Wu, A. Akhmanova, Microtubule-organizing centers. *Annu. Rev. Cell Dev. Biol.* **33**, 51–75 (2017).

2. S. Petry, R. D. Vale, Microtubule nucleation at the centrosome and beyond. *Nat. Cell Biol.* **17**, 1089–1093 (2015).

3. W. Liu, F. Zheng, Y. Wang, C. Fu, Alp7-Mto1 and Alp14 synergize to promote interphase microtubule regrowth from the nuclear envelope. *J. Mol. Cell Biol.* **11**, 944–955 (2019).

4. G. Goshima, M. Mayer, N. Zhang, N. Stuurman, R. D. Vale, Augmin: A protein complex required for centrosome-independent microtubule generation within the spindle. *J. Cell Biol.* **181**, 421–429 (2008).

5. C. M. Ho, T. Hotta, Z. Kong, C. J. Zeng, J. Sun, Y. R. Lee, B. Liu, Augmin plays a critical role in organizing the spindle and phragmoplast microtubule arrays in *Arabidopsis*. *Plant Cell* **23**, 2606–2618 (2011).

6. S. Petry, C. Pugieux, F. J. Nedelec, R. D. Vale, Augmin promotes meiotic spindle formation and bipolarity in Xenopus egg extracts. *Proc. Natl. Acad. Sci. U.S.A.* **108**, 14473–14478 (2011).

7. C. Sanchez-Huertas, F. Freixo, R. Viais, C. Lacasa, E. Soriano, J. Luders, Non-centrosomal nucleation mediated by augmin organizes microtubules in post-mitotic neurons and controls axonal microtubule polarity. *Nat. Commun.* **7**, 12187 (2016).

8. M. E. Janson, R. Loughlin, I. Loiodice, C. Fu, D. Brunner, F. J. Nedelec, P. T. Tran, Crosslinkers and motors organize dynamic microtubules to form stable bipolar arrays in fission yeast. *Cell* **128**, 357–368 (2007).

9. S. Petry, A. C. Groen, K. Ishihara, T. J. Mitchison, R. D. Vale, Branching microtubule nucleation in Xenopus egg extracts mediated by augmin and TPX2. *Cell* **152**, 768–777 (2013).

10. Y. Zhang, X. Hong, S. Hua, K. Jiang, Reconstitution and mechanistic dissection of the human microtubule branching machinery. *J. Cell Biol.* **221**, e202109053 (2022).

11. T. Murata, S. Sonobe, T. I. Baskin, S. Hyodo, S. Hasezawa, T. Nagata, T. Horio, M. Hasebe, Microtubule-dependent microtubule nucleation based on recruitment of gamma-tubulin in higher plants. *Nat. Cell Biol.* **7**, 961–968 (2005).

12. J. Luders, T. Stearns, Microtubule-organizing centres: A re-evaluation. *Nat. Rev. Mol. Cell Biol.* **8**, 161–167 (2007).

13. K. E. Sawin, P. T. Tran, Cytoplasmic microtubule organization in fission yeast. *Yeast* **23**, 1001–1014 (2006).

14. R. R. Daga, K. G. Lee, S. Bratman, S. Salas-Pino, F. Chang, Self-organization of microtubule bundles in anucleate fission yeast cells. *Nat. Cell Biol.* **8**, 1108–1113 (2006).

15. R. E. Carazo-Salas, P. Nurse, Self-organization of interphase microtubule arrays in fission yeast. *Nat. Cell Biol.* **8**, 1102–1107 (2006).

16. W. E. Borek, L. M. Groocock, I. Samejima, J. Zou, F. de Lima Alves, J. Rappsilber, K. E. Sawin, Mto2 multisite phosphorylation inactivates non-spindle microtubule nucleation complexes during mitosis. *Nat. Commun.* **6**, 7929 (2015).

17. E. M. Lynch, L. M. Groocock, W. E. Borek, K. E. Sawin, Activation of the γ-tubulin complex by the Mto1/2 complex. *Curr. Biol.* **24**, 896–903 (2014).

18. I. Samejima, V. J. Miller, S. A. Rincon, K. E. Sawin, Fission yeast Mto1 regulates diversity of cytoplasmic microtubule organizing centers. *Curr. Biol.* **20**, 1959–1965 (2010).

19. I. Samejima, V. J. Miller, L. M. Groocock, K. E. Sawin, Two distinct regions of Mto1 are required for normal microtubule nucleation and efficient association with the γ-tubulin complex in vivo. *J. Cell Sci.* **121**, 3971–3980 (2008).

20. I. Samejima, P. C. Lourenco, H. A. Snaith, K. E. Sawin, Fission yeast mto2p regulates microtubule nucleation by the centrosomin-related protein mto1p. *Mol. Biol. Cell* **16**, 3040–3051 (2005).

21. M. E. Janson, T. G. Setty, A. Paoletti, P. T. Tran, Efficient formation of bipolar microtubule bundles requires microtubule-bound γ-tubulin complexes. *J. Cell Biol.* **169**, 297–308 (2005).

22. J. Shen, T. Li, X. Niu, W. Liu, S. Zheng, J. Wang, F. Wang, X. Cao, X. Yao, F. Zheng, C. Fu, The J-domain cochaperone Rsp1 interacts with Mto1 to organize noncentrosomal microtubule assembly. *Mol. Biol. Cell* **30**, 256–267 (2019).

23. H. H. Kampinga, E. A. Craig, The HSP70 chaperone machinery: J proteins as drivers of functional specificity. *Nat. Rev. Mol. Cell Biol.* **11**, 579–592 (2010).

24. S. Zimmerman, P. T. Tran, R. R. Daga, O. Niwa, F. Chang, Rsp1p, a J domain protein required for disassembly and assembly of microtubule organizing centers during the fission yeast cell cycle. *Dev. Cell* **6**, 497–509 (2004).

25. W. Wei, B. Zheng, S. Zheng, D. Wu, Y. Chu, S. Zhang, D. Wang, X. Ma, X. Liu, X. Yao, C. Fu, The Cdc42 GAP Rga6 promotes monopolar outgrowth of spores. *J. Cell Biol.* **222**, e202202064 (2023).

26. S. Zheng, B. Zheng, Z. Liu, X. Ma, X. Liu, X. Yao, W. Wei, C. Fu, The Cdc42 GTPase-activating protein Rga6 promotes the cortical localization of septin. *J. Cell Sci.* **135**, jcs259228 (2022).

27. S. Mana-Capelli, J. R. McLean, C. T. Chen, K. L. Gould, D. McCollum, The kinesin-14 Klp2 is negatively regulated by the SIN for proper spindle elongation and telophase nuclear positioning. *Mol. Biol. Cell* **23**, 4592–4600 (2012).

28. A. Yamashita, M. Sato, A. Fujita, M. Yamamoto, T. Toda, The roles of fission yeast ase1 in mitotic cell division, meiotic nuclear oscillation, and cytokinesis checkpoint signaling. *Mol. Biol. Cell* **16**, 1378–1395 (2005).

29. I. Loiodice, J. Staub, T. G. Setty, N. P. Nguyen, A. Paoletti, P. T. Tran, Ase1p organizes antiparallel microtubule arrays during interphase and mitosis in fission yeast. *Mol. Biol. Cell* **16**, 1756–1768 (2005).

30. J. Q. Wu, T. D. Pollard, Counting cytokinesis proteins globally and locally in fission yeast. *Science* **310**, 310–314 (2005).

31. S. L. Leong, E. M. Lynch, J. Zou, Y. D. Tay, W. E. Borek, M. W. Tuijtel, J. Rappsilber, K. E. Sawin, Reconstitution of microtubule nucleation in vitro reveals novel roles for Mzt1. *Curr. Biol.* **29**, 2199–2207.e10 (2019).

32. P. T. Tran, L. Marsh, V. Doye, S. Inoue, F. Chang, A mechanism for nuclear positioning in fission yeast based on microtubule pushing. *J. Cell Biol.* **153**, 397–412 (2001).

33. S. Hua, K. Jiang, Expression and purification of microtubule-associated proteins from HEK293T cells for in vitro reconstitution. *Methods Mol. Biol.* **2101**, 19–26 (2020).

34. Z. Wang, P. Meng, X. Zhang, D. Ren, S. Yang, BON1 interacts with the protein kinases BIR1 and BAK1 in modulation of temperature-dependent plant growth and cell death in *Arabidopsis*. *Plant J.* **67**, 1081–1093 (2011).